CHAPTER 90

THREE DIMENSIONAL TESTS ON DYNAMIC EQUILIBRIUM AND ARTIFICIAL NOURISHMENT

by

J.W. Kamphuis
Professor of Civil Engineering
Queen's University, Kingston, Canada

and

R.M. Myers
Engineer, MacLaren Atlantic Ltd.
Halifax, Canada

ABSTRACT

A three dimensional facility for testing dynamic equilibrium and artificial nourishment of beaches was developed. Specific conclusions are drawn with respect to trap location and re-reflection of waves. It was found that dynamic equilibrium is achieved faster in three dimensional tests than in previous two dimensional work and that the profiles are eroding profiles rather than potential (limit) profiles. It was seen that profiles develop around the offshore bar which is shaped early in the experiments. Also the depth of the summer step was found predictable from critical shear stress considerations. Finally, onshore nourishment of eroding beaches was found to be successful.

SYMBOLS

D = particle diameter; D_{90} - 90% of the particles are smaller;

d_G = depth of water at the wave generator;

g = gravitational acceleration;

H = wave height;

n_{t_s} = sediment transport scale for wave action only (Ref. 8);

n_{t_m} = sediment transport scale for bed morphology and littoral transport;

R = runup distance; distance from SWL to maximum limit of uprush;

SWL = still water line; distance from an arbitrary measuring base line to the intersection of the still water level and the beach;

S_{SWL} = beach slope at SWL ;

T = wave period;

v_* = shear velocity;

α = angle of approach of the waves; α_G - at the wave generator; α_o - in deep water;

β = distance from the still water level to the crest of the offshore bar;

γ_s = sediment unit weight under water (= $(\rho_s-\rho)g$);

θ = distance from the still water level to the trough behind the offshore bar;

λ_b = bar distance; distance from SWL for a winter profile to the point where the bar rises suddenly out of the offshore beach slope;

λ_s = step length measured between the intersections of the summer step with the offshore beach slope and the onshore beach slope;

ν = kinematic viscosity of water;

ρ = density of water;

ρ_s = density of sediment;

Σ = distance from the still water level to the summer step;

τ_o = bottom shear stress; $(\tau_o)_c$ - critical value; $\hat{\tau}_o$ - maximum value;

INTRODUCTION

In an earlier paper (7) the first of a series of two dimensional tests on artificial beach nourishment were presented. The tests were performed on a model beach made up of the relatively coarse sand shown in Fig. 1 (D_{50} = 0.61 mm). This material was subjected to a simulated Great Lakes wave climate (neglecting tidal fluctuations and seasonal water level changes).

Since an equilibrium profile in the usual sense of the word is never achieved in the prototype, the term "dynamic equilibrium profile" was coined. Dynamic equilibrium is said to occur when a beach is acted upon long enough by a simulated, annually recurring cycle of waves so that each year, the profile returns to the same shape at the same time of year. For the simulated Great Lakes wave climate it was assumed that the total annual wave climate could be subdivided and grouped into three wave categories:

a. approximately 250 days of "background wave action", where the wave height is equal to or less than 0.3 m and the wave period of the order of 4 seconds,

b. approximately 15 days of "small storm waves" with a wave height of about 1.2 m and a wave period of 6 seconds,

c. about one and one half days of "large storm waves" with a wave height of about 3 m and a wave period 7.5 seconds.

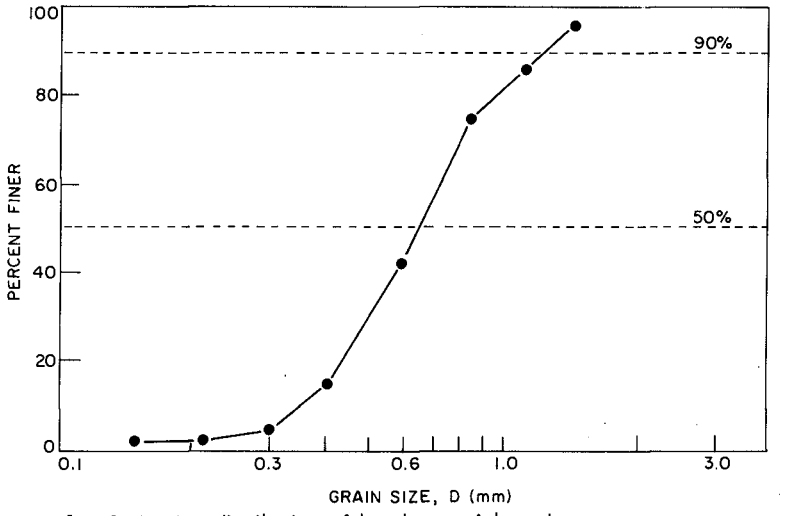

Figure 1: Grain size distribution of beach material used.

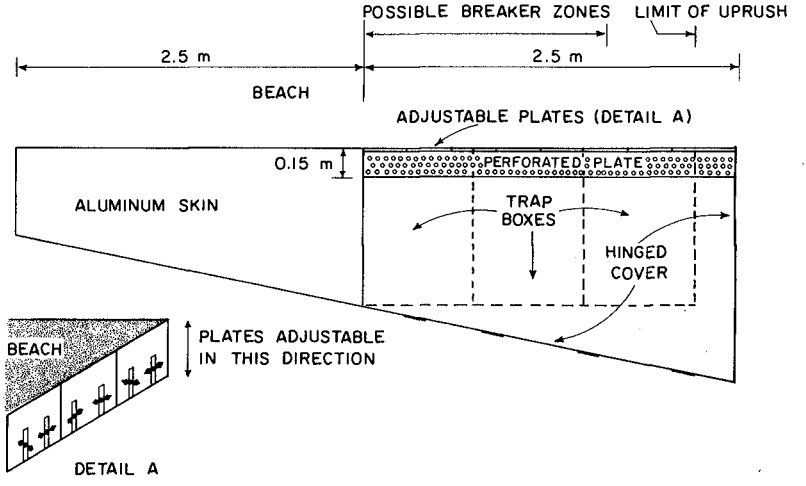

Figure 2: Sediment trap.

Although the background and small storm wave action may occur any time, the large storm waves are strictly confined to late autumn and winter. For modelling purposes, however, it was necessary to group the classes of waves together and run them in a cyclical pattern. Thus dynamic equilibrium in these studies occurs when the above wave action simulated in neat cyclical form has taken place long enough so that the profiles at the same time during each cycle are the identical. From preliminary tests it was found that the background waves moved very little or no material and thus the model wave cycle was reduced to alternate small storm waves and large storm waves. The model scale chosen was 25, i.e., the wave time scale was equal to 5. The ideal wave sediment transport time scale for two dimensional sand models (8) was found to be 210, for an assumed field particle size of 1 mm: not an unreasonable size for Great Lakes beaches under relatively heavy wave attack. Therefore the annual wave climate was simulated by a cycle of 110 minutes of 4.6 cm waves at 1.2 seconds followed by 11 minutes of 12.2 cm waves of 1.5 second period. The beaches were essentially shaped in the first five minutes of the large storm wave cycle and in the first fifteen minutes of the smaller storm wave cycle. Therefore the beach movement was correctly modelled with each of the above portions of the cycles coming to a pseudo equilibrium and errors in the estimate of sediment transport time scale resulting from the above assumptions did not result in errors in the beach profile development.

Because of the simplification of the wave climate as a two phase cycle it is difficult to define real time accurately. It may be postulated that spring or early summer occurs when the large storm wave portion of the cycle is completed. The profile resulting after the 11 minutes of large storm waves was therefore called the "winter profile". This would mean that late summer and autumn occur just before the start of the large wave portion of the cycle and thus the profile after the 110 minutes of small storm waves was called the "summer profile".

It was concluded from these earlier tests (7) that the dynamic equilibrium (even with only two phases) was much to be preferred over the normal long term equilibrium as an aid to understanding the prototype. With respect to beach nourishment, it was found that offshore nourishment (material placed seaward of the offshore bar) could be instrumental in accreting the beach as long as the material was placed in early summer and above the normal summer step level.

Nourishment placed offshore in late summer (before the large storm waves) remained trapped in the breaking zone and would not move onshore; it would only lengthen the profile. Onshore nourishment was only successful on long profiles which are normally associated with erosion. When the profile became shorter than a limiting value, called the "potential profile", onshore nourishment was totally unsuccessful. The combination of offshore nourishment to lengthen the profile and onshore nourishment yielded excellent results.

The initial impressions gained from these early tests are obviously highly incomplete without considering the presence of transport in the longshore direction as well as grain size sorting which takes place as the profile forms. Therefore, the next series of tests were performed in a three-dimensional basin. This paper is a description of the gradual development of a workable three-dimensional test basin to perform these tests and of the dynamic equilibrium achieved. Also the results of some preliminary applications of beach nourishment are described.

TEST BASIN DEVELOPMENT

Three-dimensional testing basins have been used in many studies (including Refs. 4,13,14,15,17) and each of these layouts had its own peculiarities and shortcomings as described by the various authors. At Queen's the major limitation was space, thus requiring a highly efficient sediment trapping-feeding system to give a workable beach length.

Sediment Trap

The sediment trap, as shown in Fig. 2, consisted of three boxes covered with a hinged lid, leaving a 15 cm wide slot. This slot was covered with perforated plates to allow the sediment to pass into the trap while causing as little interference as possible with the wave pattern. The leading edge of the trap (end of the beach) consisted of 30 cm long, vertically adjustable plates which were moved up and down to match the existing beach profile.

Originally the trap was placed outside of the downdrift wave guide to yield as much usable beach as possible but it was soon noted that the littoral drift was forced seaward as it approached the trap. This left a buildup of material

offshore at the downdrift end of the model causing the beach to rotate in the direction of wave approach. This phenomenon could be explained using the concept of wave set-up and set-down (2), which takes place in the basin but not over the trap (Fig. 3). The set-up, landward of the breaking zone, causes a current toward the trap while within and seaward of the breaker zone, the set-down causes a current away from the trap. By continuity, the water level at point A will be high, forcing the longshore transport to seaward. This problem was rectified by placing the trap inside the downdrift wave guide, as shown in Fig. 4, so that the trapping zone was subjected to the same set-up and set-down conditions as the remainder of the beach.

Sediment Feeder

For a short laboratory beach to behave like an infinitely long beach, the trapped material must be re-introduced with complete similarity at the upper end of the beach. This similarity must pay particular attention to variations in sediment volumes and grain size distributions with respect to distance offshore. The feeder system used in this study is shown in Fig. 5 and consisted of a conveyor belt which sheared sand from the bottom of a hopper onto a vibrating plate which in turn distributed the sand on the beach so that the waves could sort the material before it actually reached the test section.

Wave Re-reflection

Some earlier studies (4,11,14) noted that wave heights were not constant across the basin but had a tendency to increase in the downdrift direction. This was found also to be the case in this study. Most of this wave variability may be explained by re-reflection of waves within the model basin.

The incident wave in the model, as well as in the prototype, is partially reflected by the beach, resulting in a reflected wave which is approximately one order smaller than the incident wave. In the model, however, this reflected wave is re-reflected off the wave generator and the wave guides. The magnitude of this re-reflected wave depends on the quality of the wave filters used, but will be of the same order as the reflected wave. Considering only the first re-reflected wave (since subsequent reflections at the beach again reduce the wave by approximately one order) it may be seen that the simple model beach in

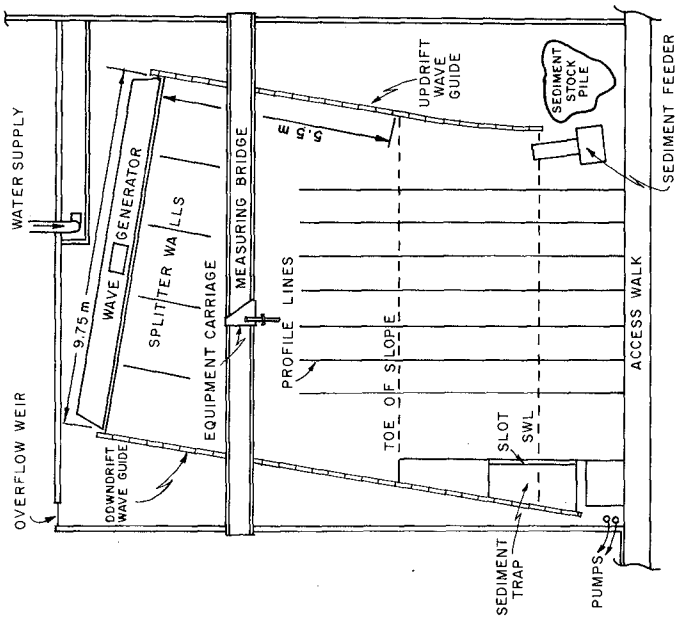

Figure 4: Basin layout.

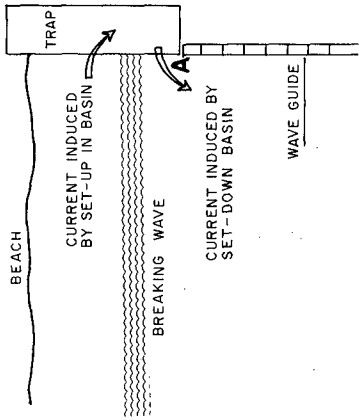

Figure 3: Induced current at trap.

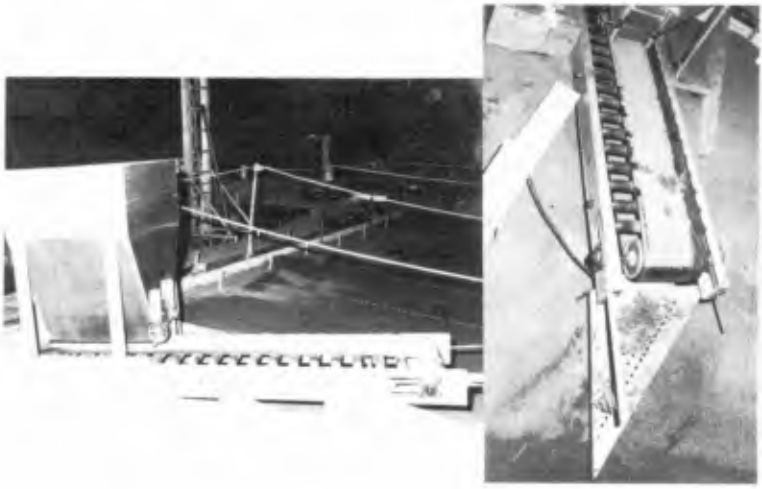

FIGURE 5: SEDIMENT FEEDER.

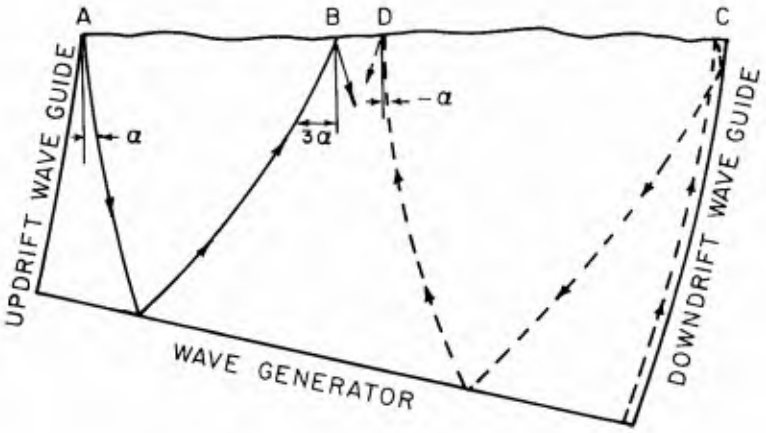

FIGURE 6: LIMITS OF RE-REFLECTED ORTHOGONALS.

Fig. 6 consists of a section AB where only the incident wave at angle α occurs (like in the prototype), a section BC where the reflected wave, re-reflected by the generator only is superimposed at an angle 3α and a further section CD where the reflected wave after suffering a double re-reflection from the wave guide and wave generator is superimposed at an angle $-\alpha$. Thus it may be expected that wave heights (and wave steepnesses) increase in the downdrift direction. This has important implications with respect to erosional patterns and the formation of the offshore bar, as shown in Fig. 7. An increase in wave height in the downdrift direction tends to rotate the model beach parallel to the wave generator. This phenomenon is completely independent from set-up problems near the trap as outlined above. Further, since littoral drift is a function of twice the angle of incidence, the littoral transport will increase considerably in the downdrift direction as a result of the large angle of incidence of the wave which is re-reflected off the generator only. In order to eliminate most of this model effect the basin was reconstructed for the last few tests to triple the shortest distance between the toe of the beach and the wave generator from 5.5 m as shown in Fig. 4 to 16.5 m. This resulted in elimination of the wave from direction 3α while the wave at $-\alpha$ came completely across the whole beach, yielding more uniform conditions. The wave splitter walls shown in Fig. 4 are also conducive to spreading the re-reflected waves more successfully across the whole basin.

THE DYNAMIC EQUILIBRIUM PROFILE

Most of the tests were carried out in the basin shown in Fig. 4. A beach consisting of 12 cm of sand (Fig. 1) laid over a concrete beach sloping at 1:10 was subjected to a simulated wave climate shown in Table 1.

TABLE 1 Simulated Great Lakes Wave Climate Used

	Duration min	H cm	T sec	d_G cm	α_G degs	α_o degs
Large Storm Waves	11	14.0	1.5	48.5	9.4	11.8
Small Storm Waves	110	4.6	1.2	48.5	9.4	10.4

where d_G is the depth of water at the wave generator
α_G is the angle between the generator and the beach
α_o is the extrapolated deep water angle of incidence

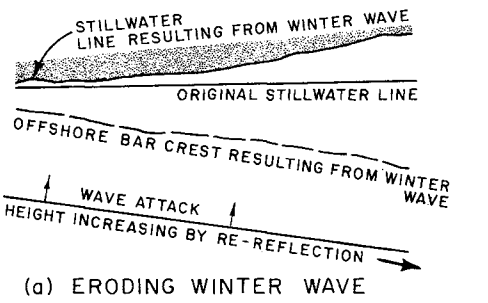

Figure 7: Effect of increasing wave height.

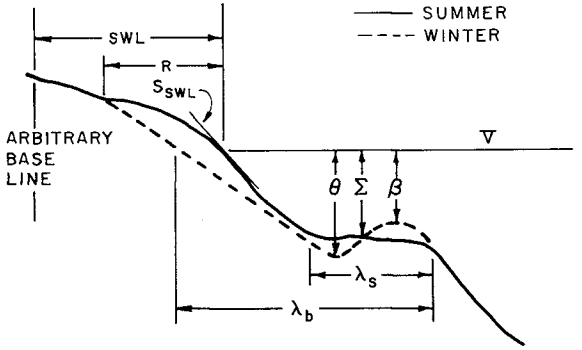

Figure 8: Profile definition.

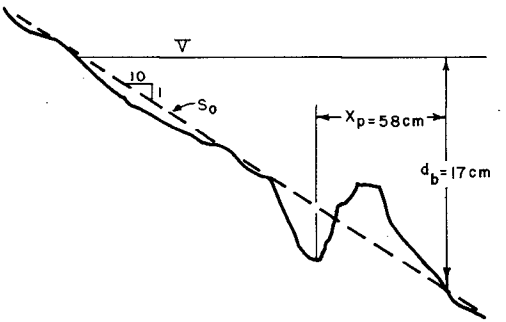

Figure 9: Beach profile after the initial half cycle of large storm waves.

Soundings were made every 5 cm and to the nearest millimeter along the profile lines in Fig. 4 after each portion of the wave cycle was completed and these profiles were plotted to determine when dynamic equilibrium was reached. An "average profile" was also plotted. This can only be done meaningfully if model is so well controlled that the beach is relatively straight and does not rotate. The profiles may be summarized by a number of key parameters shown in Fig. 8.

The first waves (large storm waves) shaped the beach so that the longshore bar was formed exactly where the breaking process takes place and Fig. 9 shows the relationship between the bar location and d_b, the depth of breaking, and X_p, the breaker travel distance, as derived using the methods of the Shore Protection Manual (16, Ch 7).

After one completed wave cycle very little change took place in the profiles and the equilibrium profiles were set up much more rapidly than in the two dimensional tests. This is a direct result of modelling the littoral processes in these tests. In the two-dimensional tests supply and removal of material could only take place in the onshore-offshore directions and a great deal of moving back and forth and balancing from cycle to cycle accomplished a final equilibrium. In the three-dimensional tests excess material was removed promptly by littoral drift and conversely, material was brought in rapidly to the areas needing supplies. The only parameter with a definite trend after one complete cycle was λ_b which slowly decreased until the seventh wave cycle. The final equilibrium parameters are listed in Table 2.

TABLE 2 Dynamic Equilibrium Parameters

Parameters Units	λ_b cm	λ_s cm	θ cm	β cm	Σ cm	SWL cm	R cm	S_{SWL}
Winter Profile	147		15.7	9.5		96	56	.21
Summer Profile		76			12.3	106	36	.20

Comparison with the two-dimensional dynamic equilibrium profiles (7) yields some interesting results. The two-dimensional λ_b was found consistently to be in the range 112 ± 10 cm. This was achieved by redistributing the 1:10

initial slope in the onshore-offshore direction using as an anchor the offshore bar which was no doubt established by the initial breakers, as in this study. The two-dimensional profile represented a "potential profile" - a limiting condition. In the three-dimensional case, however, this lengthy redistribution process was not allowed to take place since littoral transport removed all excess material quickly leaving an eroded profile with a dynamic equilibrium considerably short of the potential profile developed in the two-dimensional work. It will be seen later that upon nourishment, the potential profile is achieved. The longer λ_b also resulted in a longer λ_s in three-dimensional work. The slope at still water is somewhat greater than in the two dimensional case, again because material is removed by littoral drift. The uprush R is somewhat smaller in three dimensions because of the steeper SWL slope as well as the angle of approach of the waves. The other parameters are quite comparable.

The littoral transport during the period of larger storm waves at the time of equilibrium was .05 m^3 while for the longer period of smaller storm waves it was .13 m^3. Scaling up to prototype these figures represent a littoral drift rate of 2800 m^3/yr which is quite low for coarse beaches subjected to Great Lakes wave climates. This needs further investigation. Two factors will contribute to this low and distorted value of littoral transport. The simulation of a wave climate by grouping similar waves together as portions of cycles causes considerable scale effect in the littoral drift rate. Littoral drift is greatest at the beginning of each individual storm and decreases with time. As a result of the grouping of storms, these individual time histories are modelled by one time history, causing considerable distortion. Further, Ref. 8 gives two time scales, n_{t_s} the time scale for sediment transport by wave action only and n_{t_m} the scale for coastal morphology, and for sediment transport in the littoral direction. For this study using the assumptions mentioned earlier, the ideal time scales are

$$n_{t_s} = 210 \quad \text{and} \quad n_{t_m} = 38.4$$

The first time scale was used in the three-dimensional study for two reasons. First, it would allow comparison with the two-dimensional study. Second, although it is more likely that the second scale is the correct scale to use in the three-dimensional work, the wave durations would be increased by a factor of about 5.5.

During the experiments it was noticed that all the beach shaping took place in the first three minutes of the larger storm waves and the first 10 minutes of the smaller storm waves. Again this can be ascribed to the littoral transport effectively removing excess material and supplying depleted material rapidly. Thus it was felt that using the scale of 210 gave sufficiently long durations to model the process properly even though the term "year" might not be directly applicable. Using the second time scale, the annual littoral drift would be 15000 m^3/yr which is very close to the value observed in the field for the assumed conditions.

CRITICAL SHEAR STRESS AND THE SUMMER STEP

Since the summer step is flat in the two-dimensional as well as three-dimensional tests it was decided to use the work of Refs. 6 and 8 to determine the shear stress on the summer step to find out if a critical shear stress existed. The shear stress used is $\hat{\tau}_o$, the maximum value of the shear stress on the bottom during the wave cycle. A number of tests varying H and T were specifically run for this purpose and for 19 two-dimensional tests with wave periods in the range $0.95 \leq T \leq 2.96$ sec and wave heights $3.6 \leq H_o' \leq 6.6$ cm the mean value of the critical maximum shear stress $(\hat{\tau}_o)_c$ was 1.26 N/m^2 with a standard deviation of 0.12 N/m^2. A further six tests in the three-dimensional basin, keeping T constant at 1.2 seconds but varying H_o' from 3.3 to 5.5 cm indicated a mean value of $(\hat{\tau}_o)_c$ of 1.39 N/m^2 with a standard deviation of 0.13 N/m^2. The critical shear stress appeared to be constant. Dimensional analysis indicates for unidirectional flow that

$$\frac{(\tau_o)_c}{\gamma_s D} = f_1\left(\frac{v_* D}{\nu}\right) \tag{1}$$

which is represented by the Shields diagram. It is not unreasonable to assume that for wave motion

$$\frac{(\hat{\tau}_o)_c}{\gamma_s D} = f_2\left(\frac{\hat{v}_* D}{\nu}\right), \text{ wave-inertia interaction)} \tag{2}$$

Since only one particle size was used in these tests, other profile tests from the literature (5,10,12) and at Queen's (9,11) were used in conjunction with the methods of Refs. 6 and 8 to determine the effect of particle size. Because of armouring of the beach surface D_{90} was used in the analysis and Fig. 10 shows that

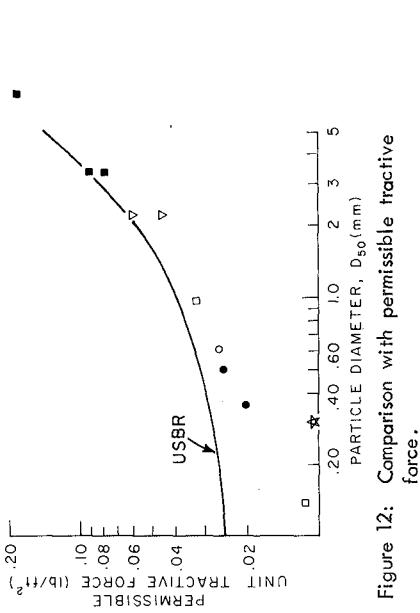

Figure 12: Comparison with permissible tractive force.

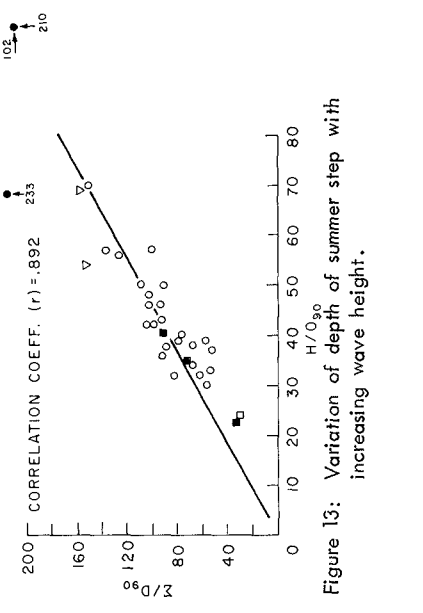

Figure 13: Variation of depth of summer step with increasing wave height.

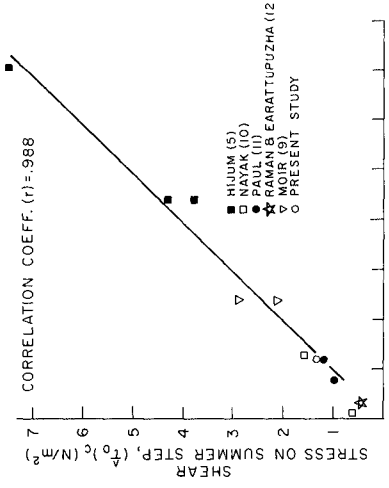

Figure 10: Critical shear stress on summer step as a function of particle size.

Figure 11: Comparison with shields curve.

$$(\hat{\tau}_o)_c = 1000\ D_{90} \tag{3}$$

in S.1. units, or

$$\frac{(\hat{\tau}_o)_c}{\gamma_s D_{90}} = 0.061 \tag{4}$$

Since $(\hat{\tau}_o)_c$ is a maximum value and considering that a number of assumptions were made about the tests performed by the other authors, this is quite close to the normal Shields condition for incipient motion at higher Reynolds numbers:

$$\frac{(\tau_o)_c}{\gamma_s D} = .05 \tag{5}$$

In order to assess the validity of the Shields criterion in this work, the points were replotted as in Fig. 11 which shows all points above the Shields line reflecting the use of the maximum value of τ_o as well as some wave-inertia effect. The points were also plotted in Fig. 12 to compare them with "critical tractive force" work (3, p 173). The USBR line implies some sediment motion and all points are below this line.

Further attempts were made to relate the summer step depth, Σ directly to wave parameters as was done by Bagnold (1) and Hijum (5). Figure 13 shows the results considering wave heights only. The scatter in this figure is mostly due to ignoring the wave period effect.

ARTIFICIAL BEACH NOURISHMENT

After dynamic equilibrium was reached and much time was expended in developing a basin, there was only time for a few nourishment tests. Although only few tests were performed, the test results will be given and these should be considered tentative until further work has been completed. In order to maximize the usefulness of the results, the winter profile was nourished in the onshore region. This had been found to be the most efficient method of nourishment under two-dimensional conditions (7). The nourishment material had the same grain size characteristics as the parent beach material (Fig. 1) but because the waves had sorted the original beach material, many of the fines had been removed from the onshore zone of the parent beach and transported offshore. Thus the nourishment material contained more fines than the native beach in the nourishment area.

The original average dynamic equilibrium, the average profile of the nourishment and the average equilibrium profiles subsequent to another 10 test cycles, are shown in Fig. 14. The test cycles were kept the same as before (including the sediment feed rate). During the first cycle after nourishment, the small storm waves eroded the new foreshore and planed off the offshore bar. This resulted in an excess of material in the summer step region, which in turn resulted in a more violent summer breaker, which yielded a summer bar corresponding to X_p and d_b of the summer wave. The new SWL slope returned to 20% immediately although the nourishment material had been placed at 29%. Figure 14 shows that no nourishment material ended up seaward of the bar and that 72% of the original nourishment remained, while the rest was removed from the test section by increased littoral drift.

The parameters for the new dynamic equilibrium are given in Table 3

TABLE 3 Dynamic Equilibrium Parameters after Nourishment

Parameters Units	λ_b cm	λ_s cm	θ cm	β cm	Σ cm	SWL cm	R cm	S_{SWL}
Winter Profile	116		11.4	8.8		119	50	.19
Summer Profile		32			12.9	128	36	.21

and comparison with Table 2 shows that λ_b has now decreased to 116 cm, close to the potential value for the two-dimensional tests. This has resulted in an attendant decrease in λ_s. Further, θ and β have both decreased indicating much more material present behind the offshore bar, SWL has moved out an average of 22.5 cm showing a net benefit at the shoreline. The other parameters remained the same.

The littoral drift during the period of larger storm waves was 0.067 m^3 while during the smaller waves it was 0.128 m^3 which makes for a total prototype drift of 3050 m^3/cycle, up slightly from the value for the initial dynamic equilibrium.

A further nourishment was subsequently applied to the dynamic equilibrium winter profile described in Fig. 14 and Table 3. During the first summer, the

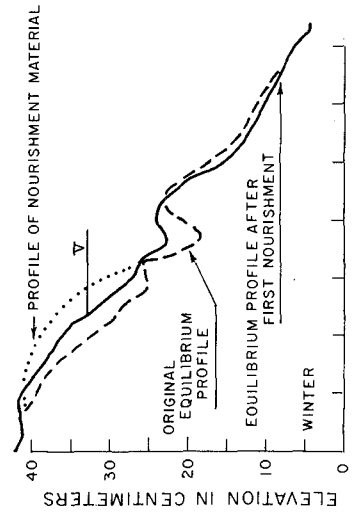

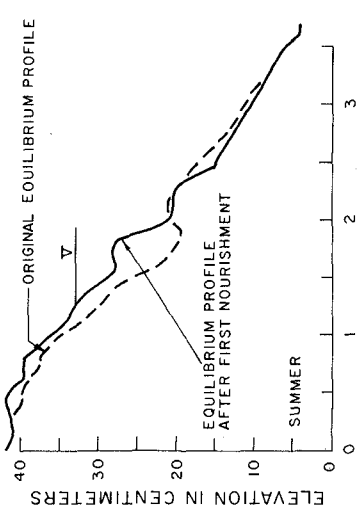

Figure 14: Summary plot of first nourishment

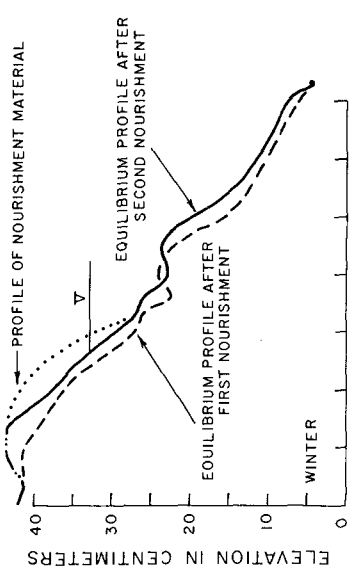

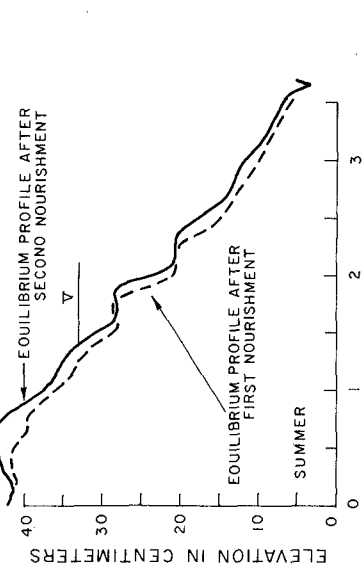

Figure 15 Summary plot of second nourishment

original nourished slope at SWL of 37% was reduced to about 20% again. The much shorter profile could not support the material eroded from the vicinity of SWL as had been the case in the previous nourishment and material was moved offshore of the existing bar. Here it was shaped by the first winter waves into a new bar 18 cm seaward of the previous bar. Equilibrium profiles occurring after a further nine cycles are given in Fig. 15 and the parameters are given in Table 4.

TABLE 4 Dynamic Equilibrium Parameters after a Second Nourishment

Parameters Units	λ_b cm	λ_s cm	θ cm	β cm	Σ cm	SWL cm	R cm	S_{SWL}
Winter Profile	113		10.9	8.5		131	51	.21
Summer Profile		31			12.6	137	34	.20

It may be seen that SWL has moved out an average distance of 10.5 cm and all other parameters are very much the same. This would indicate that the previous equilibrium profile was close to a potential profile which was shifted bodily to seaward by the nourishment. In this case only 8% of the material was removed by increased littoral drift and thus the profile behaved very much like the two-dimensional tests of Ref. 7. The littoral drift during the period of larger waves was .091 m^3 (up from the previous time) while for the period of smaller waves it was .104 m^3 (down from the previous time). The total drift still represents 3050 m^3/cycle as before.

CONCLUSIONS

With respect to development of a three-dimensional testing facility it was learned that

1. The sediment trap must be within the area subjected to wave action.
2. Wave re-reflection from the generator alone causes superimposed waves at an angle of incidence of (3α), while re-reflection from both the generator and the wave guides results in waves at angle $(-\alpha)$. The waves at $-\alpha$ cannot be avoided but the waves at 3α should be avoided in order to
    a. bring about uniform wave heights across the basin
    b. cause uniform littoral drift across the basin

c. prevent rotation of the beach in the direction of the wave generator.

With respect to dynamic equilibrium profiles it was found that

3. Dynamic equilibrium is achieved faster in three-dimensional tests.
4. The profiles resemble eroding profiles rather than potential profiles in three-dimensional tests. Potential profiles are defined as those profiles which are as short as possible.
5. The profiles develop around the offshore bar which is shaped early in the experiments at the breaking position of the large storm waves.
6. The depth to the summer step is a function of critical shear stress resulting from wave action on the beach material.

With respect to artificial beach nourishment,

7. Onshore nourishment on eroding beaches is successful.
8. Onshore nourishment on potential profiles results in a seaward shift of the whole profile.

Further study of many of these aspects is continuing at Queen's.

ACKNOWLEDGEMENTS

The funding by the National Research Council of Canada is gratefully acknowledged. Comments and suggestions by colleagues of both authors were also very helpful.

REFERENCES

1. Bagnold, R.A., "Beach Formation by Waves; Some Model Experiments in a Wave Tank", *Jour. Inst. Civil Eng., Vol 15,* 1940, pp 27-52.
2. Bowen, A.J., Inman, D.L., Simmons, V.P., "Wave Set-Down and Set-Up", *Journal of Geophysical Research, Vol 31,* 1968, pp 2569-2577.
3. Chow, V.T., *Open Channel Hydraulics,* McGraw-Hill, (1957), p 173.
4. Fairchild, J.C., "Laboratory Test of Longshore Transport", *Proceedings 12th Conference on Coastal Engineering,* Washington, 1970, pp 867-889.
5. Hijum, E.V., "Equilibrium Profiles of Coarse Material Under Wave Attack", *Proceedings 14th Conference on Coastal Engineering,* Copenhagen, 1974, pp 939-957.

6. Kamphuis, J.W., "Friction Factor Under Oscillatory Waves", *Waterways, Harbours and Coastal Engineering Journal, ASCE,* WW2, May, 1975, pp 135-144.

7. Kamphuis, J.W., Bridgeman, S.G., "Placing Artificial Beach Nourishment", *Proceedings Oceans III Conference,* Delaware, 1975, pp 197-216.

8. Kamphuis, J.W., "The Coastal Mobile Bed Model", *Queen's University, C.E. Report No. 75,* Kingston, 1975.

9. Moir, J., Ph.D. Thesis in Progress, Queen's University, Kingston, 1976.

10. Nayak, I.V., "Equilibrium Profiles of Model Beaches", *Tech. Report HEL-2-25, University of California,* 1970.

11. Paul, M.S., *"Similarity of Bed Evolution and Sediment Transport in Mobile Bed Coastal Models",* Ph.D. Thesis, Queen's University, Kingston, 1972.

12. Raman, H., Earattupuzha, J.J., "Equilibrium Conditions in Beach Wave Interaction", *Proceedings 13th Conference on Coastal Engineering,* Vancouver, 1972, pp 1237-1256.

13. Savage, R.P., "Laboratory Study of the Effect of Groins on the Rate of Littoral Transport", *Beach Erosion Board TM 114,* 1959.

14. Saville, T. Jr., "Model Study of Sand Transport Along an Infinitely Long, Straight Beach", *Transactions, American Geophysical Union, Vol 31,* 1950, pp 555-565.

15. Shay, E.A., Johnson, J.W., "Model Studies on the Movement of Sand Transported by Wave Action", Inst. of Engrg. Research, *Univ. of California, Berkeley, Issue 7, Series 14,* 1951.

16. *Shore Protection Manual,* Coastal Engineering Research Centre, 1974.

17. Swart, D.H., "Offshore Sediment Transport and Equilibrium Beach Profiles", *Publication 131, Delft Hydraulics Laboratory,* 1974.